EUROPEAN ORGANIZATION FOR NUCLEAR RESEARCH

CERN–PPE/96–042
18 March 1996

UPPER LIMIT ON THE ν_τ MASS FROM $\tau \rightarrow 3h\nu_\tau$ DECAYS

The OPAL Collaboration

Abstract

A new limit on the ν_τ mass has been determined using $Z^0 \rightarrow \tau^+\tau^-$ events selected from 140 pb^{-1} of data collected with the OPAL detector at LEP during the period 1990-1994. Using $Z^0 \rightarrow \tau^+\tau^-$ events in which both τ-leptons decay to three charged particles, a novel likelihood analysis is applied to the 2-dimensional distribution of missing mass squared and missing energy, from which we obtain a limit of $M_{\nu_\tau} <$ 35.3 MeV at 95% confidence level. Combining this result with OPAL's previous published measurement from $\tau \rightarrow 5\pi\nu_\tau$ decays, we obtain the new 95% confidence level limit of $M_{\nu_\tau} < 29.9$ MeV.

Submitted to Physics Letters B

G. Alexander[23], J. Allison[16], N. Altekamp[5], K. Ametewee[25], K.J. Anderson[9], S. Anderson[12], S. Arcelli[2], S. Asai[24], D. Axen[29], G. Azuelos[18,a], A.H. Ball[17], E. Barberio[26], R.J. Barlow[16], R. Bartoldus[3], J.R. Batley[5], G. Beaudoin[18], J. Bechtluft[14], C. Beeston[16], T. Behnke[8], A.N. Bell[1], K.W. Bell[20], G. Bella[23], S. Bentvelsen[8], P. Berlich[10], S. Bethke[14], O. Biebel[14], V. Blobel[8], I.J. Bloodworth[1], J.E. Bloomer[1], P. Bock[11], H.M. Bosch[11], M. Boutemeur[18], B.T. Bouwens[12], S. Braibant[12], P. Bright-Thomas[25], R.M. Brown[20], H.J. Burckhart[8], C. Burgard[27], R. Bürgin[10], P. Capiluppi[2], R.K. Carnegie[6], A.A. Carter[13], J.R. Carter[5], C.Y. Chang[17], C. Charlesworth[6], D.G. Charlton[1,b], D. Chrisman[4], S.L. Chu[4], P.E.L. Clarke[15], I. Cohen[23], J.E. Conboy[15], O.C. Cooke[16], M. Cuffiani[2], S. Dado[22], C. Dallapiccola[17], G.M. Dallavalle[2], C. Darling[31], S. De Jong[12], L.A. del Pozo[8], M.S. Dixit[7], E. do Couto e Silva[12], M. Doucet[18], E. Duchovni[26], G. Duckeck[8], I.P. Duerdoth[16], J.E.G. Edwards[16], P.G. Estabrooks[6], H.G. Evans[9], M. Evans[13], F. Fabbri[2], P. Fath[11], F. Fiedler[12], M. Fierro[2], H.M. Fischer[3], R. Folman[26], D.G. Fong[17], M. Foucher[17], H. Fukui[24], A. Fürtjes[8], P. Gagnon[7], A. Gaidot[21], J.W. Gary[4], J. Gascon[18], S.M. Gascon-Shotkin[17], N.I. Geddes[20], C. Geich-Gimbel[3], S.W. Gensler[9], F.X. Gentit[21], T. Geralis[20], G. Giacomelli[2], P. Giacomelli[4], R. Giacomelli[2], V. Gibson[5], W.R. Gibson[13], D.M. Gingrich[30,a], J. Goldberg[22], M.J. Goodrick[5], W. Gorn[4], C. Grandi[2], E. Gross[26], M. Gruwé[8], C. Hajdu[32], G.G. Hanson[12], M. Hansroul[8], M. Hapke[13], C.K. Hargrove[7], P.A. Hart[9], C. Hartmann[3], M. Hauschild[8], C.M. Hawkes[5], R. Hawkings[8], R.J. Hemingway[6], G. Herten[10], R.D. Heuer[8], M.D. Hildreth[8], J.C. Hill[5], S.J. Hillier[1], T. Hilse[10], P.R. Hobson[25], R.J. Homer[1], A.K. Honma[28,a], D. Horváth[32,c], R. Howard[29], R.E. Hughes-Jones[16], D.E. Hutchcroft[5], P. Igo-Kemenes[11], D.C. Imrie[25], M.R. Ingram[16], A. Jawahery[17], P.W. Jeffreys[20], H. Jeremie[18], M. Jimack[1], A. Joly[18], G. Jones[16], M. Jones[6], R.W.L. Jones[8], U. Jost[11], P. Jovanovic[1], J. Kanzaki[24], D. Karlen[6], T. Kawamoto[24], R.K. Keeler[28], R.G. Kellogg[17], B.W. Kennedy[20], J. King[13], J. Kirk[29], S. Kluth[8], T. Kobayashi[24], M. Kobel[10], D.S. Koetke[6], T.P. Kokott[3], S. Komamiya[24], R. Kowalewski[8], T. Kress[11], P. Krieger[6], J. von Krogh[11], P. Kyberd[13], G.D. Lafferty[16], H. Lafoux[21], R. Lahmann[17], W.P. Lai[19], D. Lanske[14], J. Lauber[15], J.G. Layter[4], A.M. Lee[31], E. Lefebvre[18], D. Lellouch[26], J. Letts[2], L. Levinson[26], C. Lewis[15], S.L. Lloyd[13], F.K. Loebinger[16], G.D. Long[17], B. Lorazo[18], M.J. Losty[7], J. Ludwig[10], A. Luig[10], A. Malik[21], M. Mannelli[8], S. Marcellini[2], C. Markus[3], A.J. Martin[13], J.P. Martin[18], G. Martinez[17], T. Mashimo[24], W. Matthews[25], P. Mättig[3], W.J. McDonald[30], J. McKenna[29], E.A. Mckigney[15], T.J. McMahon[1], A.I. McNab[13], F. Meijers[8], S. Menke[3], F.S. Merritt[9], H. Mes[7], J. Meyer[27], A. Michelini[8], G. Mikenberg[26], D.J. Miller[15], R. Mir[26], W. Mohr[10], A. Montanari[2], T. Mori[24], M. Morii[24], U. Müller[3], B. Nellen[3], B. Nijjhar[16], R. Nisius[8], S.W. O'Neale[1], F.G. Oakham[7], F. Odorici[2], H.O. Ogren[12], T. Omori[24], M.J. Oreglia[9], S. Orito[24], M. Palazzo[2], J. Pálinkás[33,d], J.P. Pansart[21], G. Pásztor[32], J.R. Pater[16], G.N. Patrick[20], M.J. Pearce[1], S. Petzold[27], J.E. Pilcher[9], J. Pinfold[30], D.E. Plane[8], P. Poffenberger[28], B. Poli[2], A. Posthaus[3], H. Przysiezniak[30], D.L. Rees[1], D. Rigby[1], M.G. Rison[5], S.A. Robins[13], N. Rodning[30], J.M. Roney[28], A. Rooke[15], E. Ros[8], A.M. Rossi[2], M. Rosvick[28], P. Routenburg[30], Y. Rozen[8], K. Runge[10], O. Runolfsson[8], D.R. Rust[12], R. Rylko[25], E.K.G. Sarkisyan[23], M. Sasaki[24], C. Sbarra[2], A.D. Schaile[8,e], O. Schaile[10], F. Scharf[3], P. Scharff-Hansen[8], P. Schenk[4], B. Schmitt[3], M. Schröder[8], H.C. Schultz-Coulon[10], M. Schulz[8], P. Schütz[3], J. Schwiening[3], W.G. Scott[20], T.G. Shears[16], B.C. Shen[4], C.H. Shepherd-Themistocleous[27], P. Sherwood[15], G.P. Siroli[2], A. Sittler[27], A. Skillman[15], A. Skuja[17], A.M. Smith[8], T.J. Smith[28], G.A. Snow[17], R. Sobie[28], S. Söldner-Rembold[10], R.W. Springer[30], M. Sproston[20], A. Stahl[3], M. Starks[12], K. Stephens[16], J. Steuerer[27], B. Stockhausen[3], D. Strom[19], F. Strumia[8], P. Szymanski[20],

R. Tafirout[18], H. Takeda[24], P. Taras[18], S. Tarem[22], M. Tecchio[8], N. Tesch[3], M. Thiergen[10], M.A. Thomson[8], E. von Törne[3], S. Towers[6], M. Tscheulin[10], E. Tsur[23], A.S. Turcot[9], M.F. Turner-Watson[8], P. Utzat[11], R. Van Kooten[12], G. Vasseur[21], M. Verzocchi[10], P. Vikas[18], M. Vincter[28], E.H. Vokurka[16], F. Wäckerle[10], A. Wagner[27], C.P. Ward[5], D.R. Ward[5], J.J. Ward[15], P.M. Watkins[1], A.T. Watson[1], N.K. Watson[7], P. Weber[6], P.S. Wells[8], N. Wermes[3], J.S. White[28], B. Wilkens[10], G.W. Wilson[27], J.A. Wilson[1], T. Wlodek[26], G. Wolf[26], S. Wotton[11], T.R. Wyatt[16], S. Xella[2], S. Yamashita[24], G. Yekutieli[26], K. Yoshimura[24], V. Zacek[18],

[1]School of Physics and Space Research, University of Birmingham, Birmingham B15 2TT, UK
[2]Dipartimento di Fisica dell' Università di Bologna and INFN, I-40126 Bologna, Italy
[3]Physikalisches Institut, Universität Bonn, D-53115 Bonn, Germany
[4]Department of Physics, University of California, Riverside CA 92521, USA
[5]Cavendish Laboratory, Cambridge CB3 0HE, UK
[6] Ottawa-Carleton Institute for Physics, Department of Physics, Carleton University, Ottawa, Ontario K1S 5B6, Canada
[7]Centre for Research in Particle Physics, Carleton University, Ottawa, Ontario K1S 5B6, Canada
[8]CERN, European Organisation for Particle Physics, CH-1211 Geneva 23, Switzerland
[9]Enrico Fermi Institute and Department of Physics, University of Chicago, Chicago IL 60637, USA
[10]Fakultät für Physik, Albert Ludwigs Universität, D-79104 Freiburg, Germany
[11]Physikalisches Institut, Universität Heidelberg, D-69120 Heidelberg, Germany
[12]Indiana University, Department of Physics, Swain Hall West 117, Bloomington IN 47405, USA
[13]Queen Mary and Westfield College, University of London, London E1 4NS, UK
[14]Technische Hochschule Aachen, III Physikalisches Institut, Sommerfeldstrasse 26-28, D-52056 Aachen, Germany
[15]University College London, London WC1E 6BT, UK
[16]Department of Physics, Schuster Laboratory, The University, Manchester M13 9PL, UK
[17]Department of Physics, University of Maryland, College Park, MD 20742, USA
[18]Laboratoire de Physique Nucléaire, Université de Montréal, Montréal, Quebec H3C 3J7, Canada
[19]University of Oregon, Department of Physics, Eugene OR 97403, USA
[20]Rutherford Appleton Laboratory, Chilton, Didcot, Oxfordshire OX11 0QX, UK
[21]CEA, DAPNIA/SPP, CE-Saclay, F-91191 Gif-sur-Yvette, France
[22]Department of Physics, Technion-Israel Institute of Technology, Haifa 32000, Israel
[23]Department of Physics and Astronomy, Tel Aviv University, Tel Aviv 69978, Israel
[24]International Centre for Elementary Particle Physics and Department of Physics, University of Tokyo, Tokyo 113, and Kobe University, Kobe 657, Japan
[25]Brunel University, Uxbridge, Middlesex UB8 3PH, UK
[26]Particle Physics Department, Weizmann Institute of Science, Rehovot 76100, Israel
[27]Universität Hamburg/DESY, II Institut für Experimental Physik, Notkestrasse 85, D-22607 Hamburg, Germany
[28]University of Victoria, Department of Physics, P O Box 3055, Victoria BC V8W 3P6, Canada

[29]University of British Columbia, Department of Physics, Vancouver BC V6T 1Z1, Canada
[30]University of Alberta, Department of Physics, Edmonton AB T6G 2J1, Canada
[31]Duke University, Dept of Physics, Durham, NC 27708-0305, USA
[32]Research Institute for Particle and Nuclear Physics, H-1525 Budapest, P O Box 49, Hungary
[33]Institute of Nuclear Research, H-4001 Debrecen, P O Box 51, Hungary

[a] and at TRIUMF, Vancouver, Canada V6T 2A3
[b] and Royal Society University Research Fellow
[c] and Institute of Nuclear Research, Debrecen, Hungary
[d] and Depart of Experimental Physics, Lajos Kossuth University, Debrecen, Hungary
[e] and Ludwig-Maximilians-Universität, München, Germany

1 Introduction

One of the most interesting current topics in particle physics and astrophysics is the possibility of non-zero neutrino mass. In particle physics, massive neutrinos are common features of appealing extensions of the minimal standard model, which assumes vanishing neutrino masses. The mass hierarchy between the charged and neutral leptons can be explained by the "see-saw" mechanism [1]. In this context, the τ neutrino is the best candidate to have an experimentally observable mass. In astrophysics, massive neutrinos are candidates for dark matter and may also serve as a solution for the observed deficit of solar neutrinos [2]. A heavy and unstable neutrino with mass in the MeV range, which could be directly explored by experiments at e^+e^- colliders, can have a host of interesting astrophysical and cosmological consequences [3]. The best 95% confidence level (C.L.) upper limit on the ν_τ mass M_{ν_τ} of 24 MeV has been determined by ALEPH [4], using a 2-dimensional likelihood fit to the hadronic invariant mass and hadronic total energy of 25 $\tau \to 5\pi(\pi^0)\nu_\tau$ decays.

In this letter we present an upper limit on the ν_τ mass obtained with a high statistics sample of $\tau \to 3h\nu_\tau$ decays in 3-prong versus 3-prong (3-3) $Z^0 \to \tau^+\tau^-$ events, where h is either a charged π or K meson. We employ a novel 2-dimensional likelihood technique in the plane of the missing energy and missing mass variables, which allows the extraction of a limit on the ν_τ mass using a statistical approach.

2 The OPAL detector

The OPAL detector is described in detail elsewhere [5]. Only the elements of the apparatus relevant to this analysis are described briefly here. The coordinate system is defined so that the z-axis follows the e^--beam direction and the x-y plane is perpendicular to it with the x-axis lying horizontally in the plane of the LEP ring; θ and ϕ are the usual polar coordinates. Tracking of charged particles is performed by a central tracking detector, consisting of a silicon microvertex detector, a vertex chamber, a jet chamber and z-chambers. The central tracking detector is immersed in a 0.435 T solenoidal magnetic field. The momentum resolution obtained is approximately $\sigma_p/p = \sqrt{0.02^2 + (0.0015\ p)^2}$, where p is in GeV. The silicon microvertex detector, which covers a polar angle range $|\cos\theta| < 0.83$, provided both ϕ- and z-coordinates for data taken in 1993-1994, but ϕ-coordinates only for 1991 and 1992. Only ϕ-coordinate information is used in this analysis.

The barrel electromagnetic calorimeter is located outside the magnet coil, behind an average of 2.4 radiation lengths of material. It consists of 9440 lead-glass blocks of 24.6 radiation lengths pointing toward the beam interaction region, each covering approximately 40×40 mrad^2. In the endcap there are 2264 lead-glass blocks of the same cross section but with axes parallel to the beam direction. The energy resolution is $\sigma_E/E = 2.1\%$ in the barrel and $\sigma_E/E = 3.1\%$ in the endcap for electrons with $E = 45.6$ GeV, determined from e^+e^- events.

3 Event selection

This analysis is based on a data sample of 140 pb^{-1} collected by OPAL from 1990 to 1994. To suppress effects caused by the dependence of initial state radiation on the e^+e^- center-of-mass energy, $E_{\mathrm{C.M.}}$, only data on the Z^0 peak are used (i.e. beam energies between 45.5 GeV and 45.7 GeV). The preselection of $Z^0 \to \tau^+\tau^-$ events uses the same quality cuts for charged tracks and clusters of electromagnetic energy, cosmic ray rejection, τ finding algorithm, and $q\bar{q}$ background removal used in [6]. In this preselection, the τ decay products are identified as jets of particles lying within cones of half-angle 35°; these

are referred to as "τ-jet cones" throughout this paper. A $Z^0 \to \tau^+\tau^-$ candidate must contain exactly two τ-jet cones. We use the event thrust axis to estimate the τ flight direction, and therefore in order to ensure good resolution of the thrust axis direction we require that each τ-jet cone contains precisely three charged tracks. The event thrust axis calculated from the momenta of all good charged tracks lying within the detector acceptance must satisfy $|\cos\theta_{\rm thrust}| < 0.9$. The total charge of each τ-jet cone must be ± 1 and the total charge of the event must be zero.

To remove two-photon background events, the acollinearity angle between the τ-jet cones must be less than 15°, where the directions of the jets are given by the momentum sums of the tracks and electromagnetic clusters. Residual two-photon background events are rejected by exploiting the low visible energies and very low net transverse momenta typical of $e^+e^- \to e^+e^-X$ events. An event is rejected if the sum of visible energies of the jets (taken for each jet as the larger value of the sum of track momenta and of the sum of electromagnetic cluster energies) is less than 1% of $E_{\rm C.M.}$. Further, the event is rejected if the sum of visible energy is less than 20% of $E_{\rm C.M.}$ and the missing transverse momenta, calculated separately for charged tracks and for electromagnetic clusters, are both less than 2 GeV.

Events with tracks originating from photon conversions are eliminated with an invariant mass cut of $M_{e^+e^-} < 0.05$ GeV, assuming electron masses for oppositely-charged tracks in any τ-jet cone. Tracks from $K^0 \to \pi^+\pi^-$ decays are eliminated with an invariant mass cut of $0.473\text{GeV} < M_{\pi^+\pi^-} < 0.523$ GeV, assuming π masses for the oppositely charged tracks in any τ-jet cone. A total of 1056 events in the data are rejected by the γ conversion removal cut alone, which is consistent with the expected number 1089 ± 25 from the $Z^0 \to \tau^+\tau^-$ Monte Carlo (KORALZ4.0 [7]) and 8.2 ± 5.8 events from the $q\bar{q}$ Monte Carlo (JETSET7.4 [8][9]). The Monte Carlo events were passed through a full simulation of the OPAL detector [10]. The K^0 rejection removes 34 events in the data after all other cuts, compared with 29 ± 4 events expected from $Z^0 \to \tau^+\tau^-$ and zero events from $q\bar{q}$. A total of 2354 3-3 $Z^0 \to \tau^+\tau^-$ events is selected after the above cuts. The estimates for the fractions of the different τ-decays in this preselected 3-3 $Z^0 \to \tau^+\tau^-$ event sample are listed in Table 1. The expected number of $q\bar{q}$ background events in the preselected sample is 45.1 ± 13.8 ($(1.91\pm0.58)\%$) from the Monte Carlo.

In each event, at least one τ-jet cone is required to satisfy the following requirements, aimed at selecting $\tau \to 3h\nu_\tau$ decays. To ensure well measured track momenta, the 3π energy reconstructed from the three charged tracks, $E_{3\pi}$, assuming the π mass for each track in a τ-jet cone, must satisfy $0.2 < E_{3\pi}/E_{\rm beam} < 1.2$, where $E_{\rm beam}$ is the beam energy. To suppress poorly measured tracks, the 3π mass reconstructed from the three charged track momenta $M_{3\pi} = \sqrt{{E_{3\pi}}^2 - |\vec{p}_{3\pi}|^2}$ must satisfy 0.5 GeV $< M_{3\pi} <$ 2.0 GeV. To suppress decays in which π^0s are present, we require the following:

1. the sum of electromagnetic energy in the τ-jet cone must be less than 60% of the sum of momenta of charged tracks in the τ-jet cone, Σp. This cut is sensitive to cases where the π^0 makes a relatively large contribution to the energy in the τ-jet cone.
2. the sum of electromagnetic energies in the τ-jet cone not associated with any charged track must be less than 40% of Σp. This cut is designed to reject τ-decays with an electromagnetic cluster from a π^0 which is well separated from any charged π tracks.
3. to suppress cases where a π^0 hits the same lead-glass block as a charged π track, the electromagnetic energy associated with each charged track is required to be less

Mode	Initial (%) [11]	Preselected (%)	$3h\nu_\tau$ candidates (%)
$\tau \to 3\pi\nu_\tau$	8.89	54.53 $\pm$ 0.47	76.99 $\pm$ 0.54
$\tau \to \mathrm{K K}\pi\nu_\tau$	0.17	1.16 $\pm$ 0.10	1.77 $\pm$ 0.17
$\tau \to \mathrm{K}\pi\pi\nu_\tau$	0.20	1.53 $\pm$ 0.12	2.22 $\pm$ 0.19
$\tau \to 3\pi\pi^0\nu_\tau$	5.01	27.39 $\pm$ 0.42	14.67 $\pm$ 0.46
$\tau \to 3\pi 2\pi^0\nu_\tau$	0.42	1.96 $\pm$ 0.13	0.40 $\pm$ 0.08
$\tau \to 3\pi 3\pi^0\nu_\tau$	0.06	0.25 $\pm$ 0.05	0.02 $\pm$ 0.02
non 3-prong τ-decays	85.26	12.31 $\pm$ 0.31	3.93 $\pm$ 0.25

Table 1: Decay fractions in the initial, preselected, and finally selected $\tau \to 3h\nu_\tau$ candidates, in τ MC samples.

than 80% of the charged track momentum.

After the above requirements, 2694 $\tau \to 3h\nu_\tau$ candidates are selected. From Monte Carlo simulation the selection efficiency for $\tau \to 3h\nu_\tau$ decays is (67.9$\pm$0.6)% within the preselected 3-3 topology events. The estimates for the fractions of the different τ-decays in the selected $\tau \to 3h\nu_\tau$ candidates are summarized in Table 1. The effect of small contributions from $\tau \to \mathrm{K K}\pi\nu_\tau$ and $\tau \to \mathrm{K}\pi\pi\nu_\tau$ decays is incorporated into the analysis for the $\tau \to 3h\nu_\tau$ signal as described below. The background fraction from $\mathrm{q\bar{q}}$ events is expected to be (0.46$\pm$0.26)%.

4 Method

We determine a limit on M_{ν_τ} from the distribution of the missing energy normalized by the beam energy $\omega = E_{\mathrm{miss}}/E_{\mathrm{beam}} = (E_{\mathrm{beam}} - E_{3\pi})/E_{\mathrm{beam}}$ and the missing mass squared $\eta = M^2_{\mathrm{miss}} = E^2_{\mathrm{miss}} - p^2_{\mathrm{miss}}$ for the $\tau \to 3h\nu_\tau$ candidates. The missing momentum vector $\vec{p}_{\mathrm{miss}} = \hat{p}_\tau\sqrt{E^2_{\mathrm{beam}} - M^2_\tau} - \vec{p}_{3\pi}$ is computed for each three-track decay, where $\vec{p}_{3\pi}$ is the sum of the momentum vectors of the three charged tracks, and the τ flight direction, $\hat{p}_\tau$, is estimated using the event thrust axis direction, $\hat{p}_{\mathrm{thrust}}$. The vector $\hat{p}_{\mathrm{thrust}}$ is calculated from the sum of the three-track momentum vectors $\vec{p}_{3\pi}$ and $\vec{p}\,'_{3\pi}$ for the two τ-decays: $\hat{p}_{\mathrm{thrust}} = (\vec{p}_{3\pi} - \vec{p}\,'_{3\pi})/|\vec{p}_{3\pi} - \vec{p}\,'_{3\pi}|$. The use of the variable M^2_{miss} is a new feature of this analysis. A non-zero $M^2_{\nu_\tau}$ contributes directly to M^2_{miss}. The M^2_{miss} peak becomes broadened because of the assumption that the τ flight direction is the thrust axis, as can be seen from the expression $M^2_{\mathrm{miss}} = M^2_{\nu_\tau} + 2p_\tau p_{3\pi}(\cos\Psi_{\mathrm{thrust}} - \cos\Psi_\tau)$, where Ψ_{thrust} and Ψ_τ are the event thrust axis and the true τ flight direction angles with respect to the $\vec{p}_{3\pi}$ decay. The event thrust axis direction typically differs from the true τ flight direction by 7 mrad in 3-3 $\mathrm{Z}^0 \to \tau^+\tau^-$ events due to the recoil of ν_τ. This is the dominant contribution to the observed width of M^2_{miss} and can be predicted by the Monte Carlo for a given input value for M_{ν_τ}. The observed η and ω distributions from the selected $\tau \to 3h\nu_\tau$ data and Monte Carlo samples are shown in Figure 1. The agreement is reasonable: it should be noted that the analysis method does not rely on the Monte Carlo to model these distributions; instead the resolution function is determined from data, as explained below.

The distribution of data in the 2-dimensional (η, ω) plane is compared to that predicted by Monte Carlo samples in which the ν_τ is assigned various masses and the detector resolution and acceptance effects are included. We perform a cone-by-cone maximum likelihood fit to extract the best value for M_{ν_τ}. The likelihood for each selected $\tau \to 3h\nu_\tau$

candidate i takes the form:

$$\mathcal{L}_i(M_{\nu_\tau},\eta_i,\omega_i) = \frac{\int \mathrm{d}\eta \int \mathrm{d}\omega\ \mathcal{P}(M_{\nu_\tau},\eta,\omega)\ \mathcal{D}(\eta-\eta_\mathrm{i},\omega-\omega_\mathrm{i},\sigma_{\eta_\mathrm{i}},\sigma_{\omega_\mathrm{i}},\rho_\mathrm{i})}{\int \mathrm{d}\eta \int \mathrm{d}\omega\ \{\ \mathcal{P}(M_{\nu_\tau},\eta,\omega) \int \mathrm{d}\eta' \int \mathrm{d}\omega'\ \mathcal{D}(\eta-\eta',\omega-\omega',\sigma_{\eta_\mathrm{i}},\sigma_{\omega_\mathrm{i}},\rho_\mathrm{i})\}}\ ,$$

where $\mathcal{P}$ is the physics function, $\mathcal{D}$ is the detector resolution function, σ_η, σ_ω, and ρ are the errors and correlation coefficient for η and ω. These last three variables are obtained from track parameters and error matrices of the i-th 3π decay candidate, assuming all charged decay products are pions. The physics function is defined for the region -1 GeV$^2 < \eta <$ 1 GeV^2 and $0 < \omega < 1$. The cut $|\eta_i| < 1$ GeV^2 is also applied to measured candidates. A total of 2514 $\tau \to 3h\nu_\tau$ candidates are left after this cut.

The physics function consists of a term for $\mathrm{Z}^0 \to \tau^+\tau^-$ events and one for non-τ background events. We consider $\mathrm{q\bar{q}}$ events to be the only non-τ background, and their distribution is independent of the true M_{ν_τ}. The physics function can be written as:

$$\mathcal{P}(M_{\nu_\tau},\eta,\omega) = (1-f_{\mathrm{q\bar{q}}})\mathcal{P}_{\tau\tau}(M_{\nu_\tau},\eta,\omega) + f_{\mathrm{q\bar{q}}}\mathcal{P}_{\mathrm{q\bar{q}}}(\eta,\omega) \quad ,$$

where $f_{\mathrm{q\bar{q}}}$ is the fraction of $\mathrm{q\bar{q}}$ events in the selected sample. A JETSET7.4 event sample with full detector simulation was used to obtain $\mathcal{P}_{\mathrm{q\bar{q}}}(\eta,\omega)$; the full simulation was needed in order to determine the acceptance, but the true particle momenta were used to define η and ω, since in the fit these are convolved with the detector resolution function $\mathcal{D}$. To include the effect of the correlations between the two τ-jet cones through the thrust axis direction, the 2-dimensional physics function $\mathcal{P}_{\tau\tau}$ has separate contributions from $3h$ and $3h\mathrm{n}\pi^0$ ($\mathrm{n}\geq 1$) decay modes in each τ-jet cone. The function $\mathcal{P}_{\tau\tau}$ for a candidate $\tau \to X\nu_\tau$ decay is given by:

$$\mathcal{P}_{\tau\tau}(M_{\nu_\tau},\eta,\omega) = \sum_{X,X'} f_X f_{X'} \mathcal{T}_{X,X'}(M_{\nu_\tau},\eta,\omega)\epsilon_X(\eta,\omega) + \mathcal{P}_{non3}(\eta,\omega) \quad ,$$

where f_X is is the decay fraction of τ into 3-prong decays in the sample of $\tau \to 3h\nu_\tau$ candidates and $f_{X'}$ is the corresponding fraction in the opposite τ-jet cone (X, X'=$3h$ or $3h\mathrm{n}\pi^0$), $\epsilon_X(\eta,\omega)$ is the normalized efficiency function ($\int\int \mathrm{d}\eta\mathrm{d}\omega\epsilon_\mathrm{X} = 1$) for the $\tau \to X\nu_\tau$ decay, $\mathcal{T}_{X,X'}(M_{\nu_\tau},\eta,\omega)$ is the theoretical distribution for $\tau \to X\nu_\tau$ decays with $\tau \to X'\nu_\tau$ in the opposite τ-jet cone, and $\mathcal{P}_{non3}(\eta,\omega)$ is the contribution to the physics function from events with background sources other than 3-prong τ decays in either τ-jet cone. Some 1-prong decays, such as $\tau \to \rho\nu_\tau$ and $\tau \to \mathrm{K}^*\nu_\tau$, survive the 3π selection through photon conversions. The contribution from these backgrounds is expected to have negligible sensitivity to M_{ν_τ} because of large fluctuations on the plane of (η,ω) and the small fraction of these events in the final sample. The functions $\mathcal{T}_{X,X'}(M_{\nu_\tau},\eta,\omega)$ are obtained from the theoretical decay distributions on the (η, ω) plane taking account of the bias from the thrust axis direction, using X, X' events without detector simulation generated with KORALZ4.0 in steps of 10 MeV for M_{ν_τ} and including multiple initial and final state photon radiation. The functions $\epsilon_X(\eta,\omega)$, $\mathcal{P}_{non3}(\eta,\omega)$, are estimated from KORALZ4.0 event samples with full detector simulation. The dependence of $\epsilon_X(\eta,\omega)$ on ω for $\tau \to 3h\nu_\tau$ decays is relatively small, while the $\tau \to 3h\mathrm{n}\pi^0\nu_\tau$ decays with large ω are suppressed by the π^0 rejection cuts. In Figures 2 a)-d), contour plots of reference histograms of the physics functions are shown. The region of greatest sensitivity lies around the peak in η and near the end-point of $\omega = 0$. From these plots one can also observe the good separation on the (η,ω) plane between the contributions from $3h$ and $3h\mathrm{n}\pi^0$ decays. Furthermore, the fit for M_{ν_τ} to the 2-dimensional distribution can substantially reduce the systematic uncertainties in the measured M_{ν_τ} arising from the momentum scale, resolution, and beam

energy, because of the different sensitivities of the two correlated variables (η, ω) to these effects.

The detector resolution function is given by the 2-dimensional Gaussian distribution: $\mathcal{D}(\eta - \eta_i, \omega - \omega_i, \sigma_{\eta_i}, \sigma_{\omega_i}, \rho_i)$. The experimental resolutions strongly depend on the properties of specific events (*e.g.* presence of z-chamber or silicon microvertex detector hits). In order to take this into account, the resolutions σ_{η_i} and σ_{ω_i} and the correlation coefficient ρ_i are individually reconstructed for each of the selected $\tau \to 3h\nu_\tau$ candidates using the track parameters and their respective error matrices. These resolutions depend on the track parameters in both τ-jet cones, because of the dependence of η_i on the thrust axis direction. We emphasize again that the resolution used to estimate the likelihood is taken from data, not Monte Carlo. The distributions of σ_{η_i} and σ_{ω_i} have peaks at 0.03 GeV^2 and 0.01, respectively, which are lower than their average values, 0.10 GeV^2 and 0.02.

Each of the track error matrix elements is corrected by a scaling factor determined from $Z^0 \to \mu^+\mu^-$ events after correcting for the effects of initial state radiation and the center-of-mass energy spread. The systematic uncertainty on the scaling factors is estimated to be 4% using $D^* \to K\pi\pi$ decays as described below. To improve the resolution of η, the three tracks are constrained to a reconstructed secondary vertex if one can be formed with χ^2-probability $> 1\%$. Only 14% of the selected $\tau \to 3h\nu_\tau$ decays do not meet this requirement. The η resolution is, on average, 0.09 GeV^2 for the $\tau \to 3h\nu_\tau$ decays with a good vertex and 0.18 GeV^2 for the decays without a good vertex and therefore the events without a good vertex carry little statistical weight in the fit.

5 Results

Using the 2-dimensional likelihood technique described in Section 4, we estimate the total likelihood values for the 2514 selected $\tau \to 3h\nu_\tau$ candidates as the assumed true M_{ν_τ} is changed from 0 MeV to 150 MeV in 10 MeV steps. The results of these total likelihood values favour M_{ν_τ}=0 MeV as shown in Figure 3 a). To obtain an upper limit on M_{ν_τ}, we considered the following three different approaches:

1. We fit the likelihood distribution as a function of M_{ν_τ} using a third order polynomial multiplied by a Gaussian (Figure 3 a)). By integrating the function over the physical region, we obtain an upper limit at 95% C.L., $M_{\nu_\tau} < 32.1$ MeV.
2. We fit the likelihood distribution as a function of $M^2_{\nu_\tau}$ using a Gaussian, which has the advantage that the likelihood parameterization can be extrapolated into the unphysical region. The peak of the Gaussian lies at negative $M^2_{\nu_\tau}$, but is statistically consistent with the assumption of zero mass. The 95% C.L. limit on M_{ν_τ} is $M_{\nu_\tau} <$ 33.6 MeV, constraining $M^2_{\nu_\tau} > 0$ MeV^2.
3. We form the distribution of $\Delta \ln \mathcal{L} = \ln \mathcal{L}(0) - \ln \mathcal{L}(M_{\nu_\tau})$ and obtain a 95% C.L. limit by noting the value of M_{ν_τ} at which $\Delta \ln \mathcal{L} = 1.92$. The 95% C.L. limit is $M_{\nu_\tau} < 31.7$ MeV.

For our quoted limit, we use the first approach and consider the others as consistency checks. The second approach verifies that the limit is sensitive neither to the assumption of uniform *a priori* probability in M_{ν_τ} or $M^2_{\nu_\tau}$, nor to the details of the fit parameterization used. The third approach finds that value of M_{ν_τ} that, if it were the true value, would result in a probability of 95% to measure a smaller difference between $\ln \mathcal{L}(M_{\nu_\tau})$ and the observed maximum of $\ln \mathcal{L}$, if the experiment were to be repeated many times. Although having a different meaning, this value lies close to the results of the other two approaches.

This raw result must be corrected for the following systematic effects:

- **Beam energy**: The absolute beam energy, used to calculate the τ momentum in the determination of η, is varied by its uncertainty of 6.0 MeV, as determined by the working group on LEP energy [12].
- **τ mass**: The value of the τ mass M_τ= 1777.02 MeV, used to calculate the τ momentum p_τ in the determination of η, is varied by its present total error of 0.30 MeV [13].
- **M_{a_1} and Γ_{a_1}**: For the reference histograms of the physics functions and the Monte Carlo events with full-detector simulation, M_{a_1} and Γ_{a_1} are set to 1.251 GeV and 0.599 GeV respectively. These values are obtained from fits to ARGUS data for the a_1 spectral function assuming the same theoretical model for the partial decay rate of a_1 [15] as is implemented in KORALZ4.0. They are also consistent with the recent OPAL measurement [14]. The errors in the determination of M_{a_1} and Γ_{a_1}, 13 MeV and 44 MeV, which are also taken from [15], are used as systematic uncertainties for M_{a_1} and Γ_{a_1} in the Monte Carlo. To evaluate the uncertainty due to M_{a_1}, we generated another set of reference histograms using an input M_{a_1} shifted by 13 MeV and observed the limit variation from this shift. A similar technique was used in order to estimate the systematic uncertainty arising from the error on Γ_{a_1}.
- **Decay fractions in the final sample**: The absolute uncertainties for the final fractions of $3h\mathrm{n}\pi^0$, non 3-prong, and $\mathrm{q\bar{q}}$ are estimated to be 1.5%, 0.3%, and 0.4%, respectively, as follows. For the $3h\mathrm{n}\pi^0$ component, a control sample enriched in such decays was used to assess the consistency between data and Monte Carlo for the $3h\mathrm{n}\pi^0$ rejection cuts. The uncertainty in the $3h\mathrm{n}\pi^0$ branching ratio [11] was also taken into account. For the non 3-prong decays, the difference between the photon conversion rates in data and Monte Carlo, and the Monte Carlo statistical error, were taken into account. The uncertainty in the $\mathrm{q\bar{q}}$ background was estimated using a control sample enriched in $\mathrm{q\bar{q}}$ events.
- **Normalized efficiency function**: The uncertainty in the slope of the ω-dependence of the efficiency function is conservatively estimated to be $\pm 0.20\omega$. Changing the slope by this amount has negligible influence on the 95% C.L. limit.
- **Resolutions**: From cross checks with a $\mathrm{D}^* \to \mathrm{K}\pi\pi$ sample, we find that the width of the $M_{\mathrm{D}^*}/\sigma(M_{\mathrm{D}^*})$ distribution from D^* decays is consistent with unity within the statistical error of 4% after the background subtraction. An uncertainty of 4% is taken.
- **Momentum, θ, and ϕ offset**: The absolute momentum uncertainty is estimated to be less than 0.25% from the μ^- and μ^+ momentum distribution in $\mathrm{Z}^0 \to \mu^+\mu^-$ events, which is essentially due to calibration effects. The offset is expected to be smaller for low momentum tracks. Furthermore, the measurements of the D^0 and the D^+ mass are sensitive to such systematics, particularly multi-track effects. We have measured the mass of D^0 and D^+ from $\mathrm{D}^0 \to \mathrm{K}^-\pi^+$ and $\mathrm{D}^+ \to \mathrm{K}^-\pi^+\pi^+$ decays and the discrepancies from the world average values [16] are (0.016 ± 0.054)% and (0.145 ± 0.064)%, respectively. The sums in quadrature of the discrepancies and the errors, 0.056% and 0.158%, can be converted into corresponding measured momentum uncertainties of 0.07% and 0.17%, which are lower than our estimate of 0.25% for the momentum offset. Possible offsets of θ and ϕ are also estimated by observing the acollinearity angle in $\mathrm{Z}^0 \to \mu^+\mu^-$ events. The uncertainties are 0.2 mrad for both angles. The variations in the limits for M_{ν_τ} are investigated as momenta, θ, and ϕ angle of tracks are changed, independently, by amounts corresponding to the above offsets in the process of reconstruction of M^2_{miss}, E_{miss}, and their covariances.

Source	uncertainty	limit variation (MeV)
$E_{\rm beam}$	6 MeV	0.1
M_τ	0.30 MeV	< 0.1
$\mathrm{M_{a_1}}$	13 MeV	0.8
$\Gamma_{\mathrm{a_1}}$	44 MeV	1.2
$f_{3h\mathrm{n}\pi^0}$	1.5 %	0.6
f_{non3}	0.3 %	0.1
$f_{\mathrm{q\bar{q}}}$	0.4 %	< 0.1
$\epsilon_{3h\mathrm{n}\pi^0}(\eta,\omega)$	20 %	< 0.1
resolution	4 %	1.2
momentum offset	0.25%	2.2
θ offset	0.2 mrad	0.1
ϕ offset	0.2 mrad	0.1
$M^2_{\rm miss}$ cuts		1.2
total		3.2

Table 2: List of systematic errors. The variation of the 95% C.L. M_{ν_τ} limit is shown for each systematic source.

- **Cuts in $M^2_{\rm miss}$**: In the distribution of $M^2_{\rm miss}$, the tail in the region of -0.6 GeV^2 $< M^2_{\rm miss} < -0.4$ GeV^2 is not modelled well by Monte Carlo (See Figure 1 a)). A tighter cut of -0.4 GeV^2 $< M^2_{\rm miss} <$ 1.0 GeV^2 was used and the number of candidates decreased by 186. The limit increases by 3.8 MeV if the 186 candidates are removed. From τ Monte Carlo events with the same statistics, the tighter cut removes 111 candidates and the variation in the limit is 3.5 MeV. We take 1.2 MeV as an uncertainty from the tail by subtracting 3.5 MeV and 3.8 MeV in quadrature.

The variations in the 95% C.L. M_{ν_τ} limit for each systematic source are listed in Table 2. Assuming that the above systematic errors are independent of each other, the total systematic error in the M_{ν_τ} measurement is estimated from adding them in quadrature. The result of 3.2 MeV is added linearly to the raw upper limit to form the corrected value:

$$M_{\nu_\tau} < 35.3 \text{ MeV}, \quad 95\% \text{ C.L.}$$

6 Cross checks

The sensitivity of the fit to a massive ν_τ is investigated with dedicated samples of Monte Carlo events with full detector simulation in which M_{ν_τ} is set to 50 and 100 MeV and about 3500 τ-decays remain after selection cuts. The results of the likelihood fits are 47^{+18}_{-23} MeV and 104^{+11}_{-14} MeV, respectively. With about 7000 decays the results are 55^{+12}_{-16} MeV and 108^{+6}_{-7} MeV, respectively.

We have also fitted the data for M_{ν_τ} in the 1-dimensional ω distributions using the same likelihood scheme presented in Section 4 but simplified. For this fit using the observed ω distribution, only 394 $\tau \to 3h\nu_\tau$ decays in the region of $-0.1 < \omega_i < 0.1$ are used, and so the fractions f_X are reestimated. The result of the likelihood fit is consistent with $M_{\nu_\tau} = 0$ MeV and the 95% C.L. limit is obtained at 86 MeV. Furthermore, a higher statistics check is done using 2579 $\tau \to 3h\nu_\tau$ decays in 1-3 $\mathrm{Z^0} \to \tau^+\tau^-$ events. Again we observe consistency with M_{ν_τ}=0 MeV and the 95% C.L. limit of 59 MeV. The uncertainty in the measured momentum offset of 0.25%, as described in Section 6, corresponds to a

systematic shift of the likelihood peak by 70 MeV in this 1-dimensional analysis. This kind of systematic variation is substantially reduced in the 2-dimensional likelihood technique.

The framework of the fitting scheme, scaling factors, and systematics of detector response are checked by measuring the τ lifetime using the vertex separation of 3-3 $Z^0 \to \tau^+\tau^-$ events. The measured value is 292.4 ± 8.3 fs, where the error is statistical only, in agreement with the most recent OPAL published value of 289.2 ± 2.1 fs [17] and the world average 295.6 ± 3.1 fs [18].

7 Conclusions

We obtain an upper limit of $M_{\nu_\tau} < 35.3$ MeV at the 95% C.L. from 2514 $\tau \to 3h\nu_\tau$ candidates in the 3-3 topology of $Z^0 \to \tau^+\tau^-$ through a comparison of the 2-dimensional distribution of missing mass squared and missing energy with theoretical predictions as a function of M_{ν_τ}.

The likelihood curve for this analysis combined with the published OPAL measurement from $\tau \to 5\pi\nu_\tau$ decays [19], obtained by multiplying raw likelihoods from both measurements at the same M_{ν_τ} points, is shown in Figure 3 b). From these new likelihood values as a function of M_{ν_τ}, we find a combined upper limit for M_{ν_τ} without correcting for the above systematic uncertainties of $M_{\nu_\tau} < 26.7$ MeV at the 95% C.L. After adding the total systematic variation in this analysis to the combined raw upper limit, the final combined limit on M_{ν_τ} is found to be:

$$M_{\nu_\tau} < 29.9 \text{ MeV}, \quad 95\%\text{C.L.}$$

8 Acknowledgements

It is a pleasure to thank the SL Division for the efficient operation of the LEP accelerator, the precise information on the absolute energy, and their continuing close cooperation with our experimental group. In addition to the support staff at our own institutions we are pleased to acknowledge the
Department of Energy, USA,
National Science Foundation, USA,
Particle Physics and Astronomy Research Council, UK,
Natural Sciences and Engineering Research Council, Canada,
Israel Ministry of Science,
Israel Science Foundation, administered by the Israel Academy of Science and Humanities,
Minerva Gesellschaft,
Japanese Ministry of Education, Science and Culture (the Monbusho) and a grant under the Monbusho International Science Research Program,
German Israeli Bi-national Science Foundation (GIF),
Direction des Sciences de la Matière du Commissariat à l'Energie Atomique, France,
Bundesministerium für Bildung, Wissenschaft, Forschung und Technologie, Germany,
National Research Council of Canada,
Hungarian Foundation for Scientific Research, OTKA T-016660, and OTKA F-015089.

References

[1] T. Yanagida, *Proceedings of the Workshop on the Unified Theory and the Baryon Number in the Universe*, ed. by O. Sawada and A. Sugamoto, KEK(1979) 95;

M. Gell-Mann, P. Ramond and R. Slansky, *Supergravity*, ed. by D. Freedman et al., North Holland (1979).
[2] S.P. Rosen and J.M. Gelb, Phys. Rev. D34 (1986) 969;
H.A. Bethe, Phys. Rev. Lett. 56 (1986) 1305.
[3] G. Gyuk and M. Turner, Nucl. Phys. B, Proc. Suppl. 40 (1995) 557.
[4] ALEPH Collab., D Buskulic, et al., Phys .Lett. B349 (1995) 585.
[5] OPAL Collab., K. Ahmet et al., Nucl. Inst. and Meth., A313 (1992) 103;
P. Allport et al., Nucl. Inst. And Meth., A324 (1993) 34;
P. Allport et al., Nucl. Inst. And Meth., A346 (1994) 476.
[6] OPAL Collab., G. Alexander et al., Phys. Lett. B266 (1991) 201.
[7] S. Jadach, J.H. Kühn and Z. Was, Comp. Phys. Comm., 64, (1991) 275.
[8] T. Sjöstrand, Comp. Phys. Comm. 39 (1986) 347;
T. Sjöstrand and M. Bengtsson, Comp. Phys. Comm. 43 (1987) 367;
T. Sjöstrand, CERN-TH.6488/92.
[9] The JETSET 7.4 parameters were tuned as described in
OPAL Collab., G. Alexander et al., CERN-PPE/95-126.
[10] J. Allison et al., Nucl. Inst. And Meth., A317 (1992) 47.
[11] New averages were formed including the following results. The weighted means were calculated with the constraint that all branching ratios had to add up to one:
Particle Data Group, τ^- *BRANCHING RATIOS*, Phys. Rev. D50 (1994) 1407;
ALEPH Collab., D. Buskulic et al., Phys. Lett. B332 (1994) 209;
ALEPH Collab., D. Buskulic et al., Phys. Lett. B332 (1994) 219;
CLEO Collab., M. Battle et al., CLNS/94/1273;
DELPHI Collab., P. Abreu et al., CERN-PPE/94-88;
OPAL Collab., R. Akers et al., Phys. Lett. B339 (1994) 278;
OPAL Collab., R. Akers et al., Z. Phys. C66 (1995) 543.
[12] The working group on LEP energy, Phys. Lett. B307 (1993) 187.
[13] BES Collab., J.Z. Bai et al., Phys. Rev. D53 (1996) 20.
[14] OPAL Collab., R. Akers et al., Z. Phys. C67 (1995) 45.
[15] J.H. Kühn and A. Santamaria, Z. Phys. C48 (1990) 445.
[16] Particle Data Group, $D^{\pm}$ *MASS*, Phys. Rev. D50 (1994) 1572;
Particle Data Group, D^0 *MASS*, Phys. Rev. D50 (1994) 1581.
[17] OPAL Collab., R. Akers et al., to appear in Phys. Lett. B, CERN-PPE/96-018 (1996).
[18] Particle Data Group, τ^- *MEAN LIFE*, Phys. Rev. D50 (1994) 1404.
[19] OPAL Collab., R. Akers et al., Z. Phys. C65 (1995) 183.

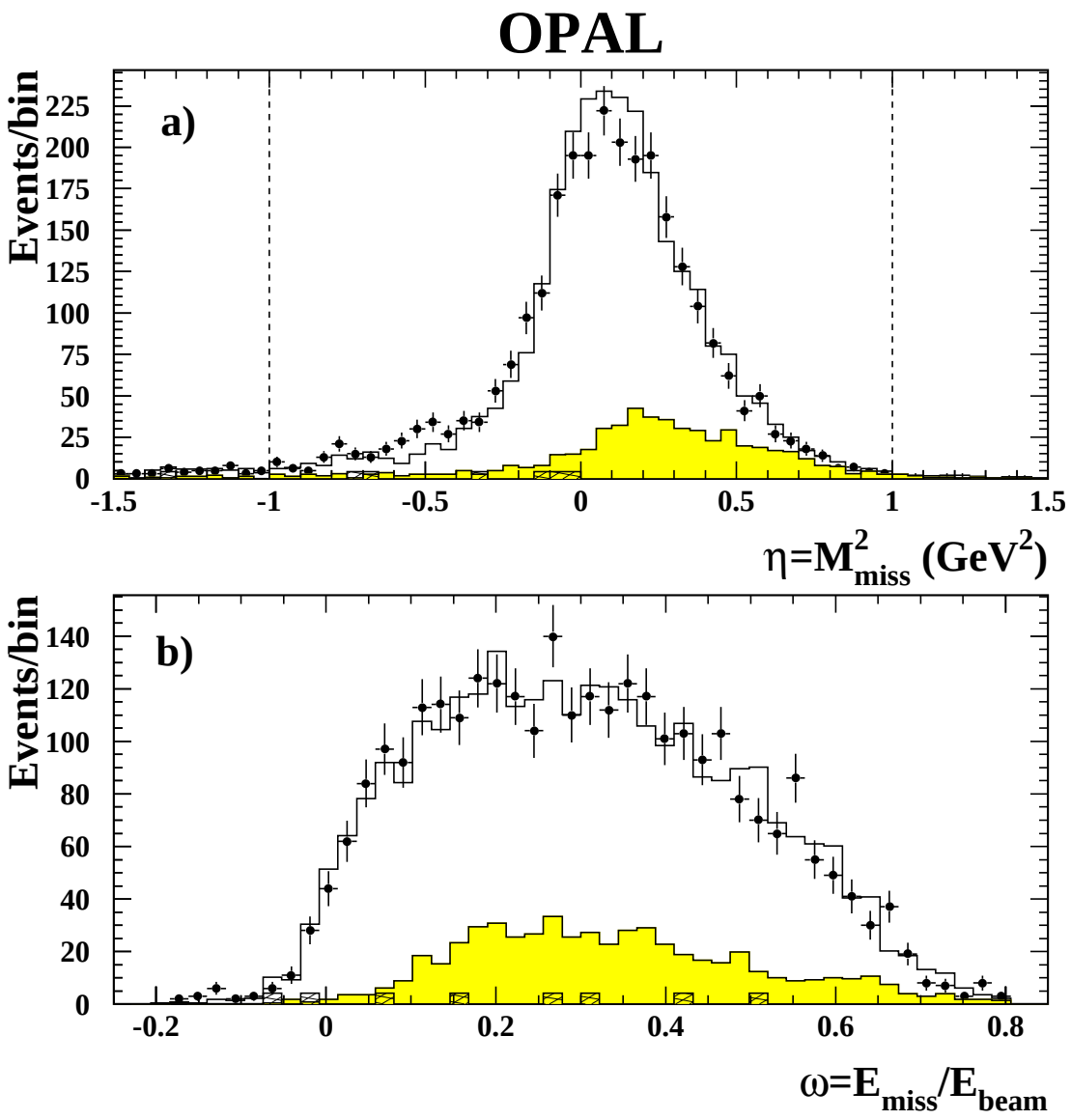

Figure 1: Distributions of a) reconstructed $\eta{=}M^2_{\rm miss}$ in GeV^2 and b) reconstructed $\omega{=}E_{\rm miss}/E_{\rm beam}$ after all selection cuts except the cut $|M^2_{\rm miss}| < 1$GeV^2 are imposed for $\tau \to 3h\nu_\tau$ candidates in the data and Monte Carlo τ and q$\bar{\rm q}$ events. Data are represented as points with error bars. Monte Carlo expectations at $M_{\nu_\tau}{=}10$ MeV are shown as the solid histogram. The $3hn\pi^0$ and non 3-prong decays are shown as the shaded histogram. The q$\bar{\rm q}$ background expectation is shown as the hatched histogram. The cut $|M^2_{\rm miss}| < 1$GeV^2 is shown as dashed lines on the $\eta{=}M^2_{\rm miss}$ plots. Monte Carlo predictions are normalized to the number of preselected 3-3 $Z^0 \to \tau^+\tau^-$ events.

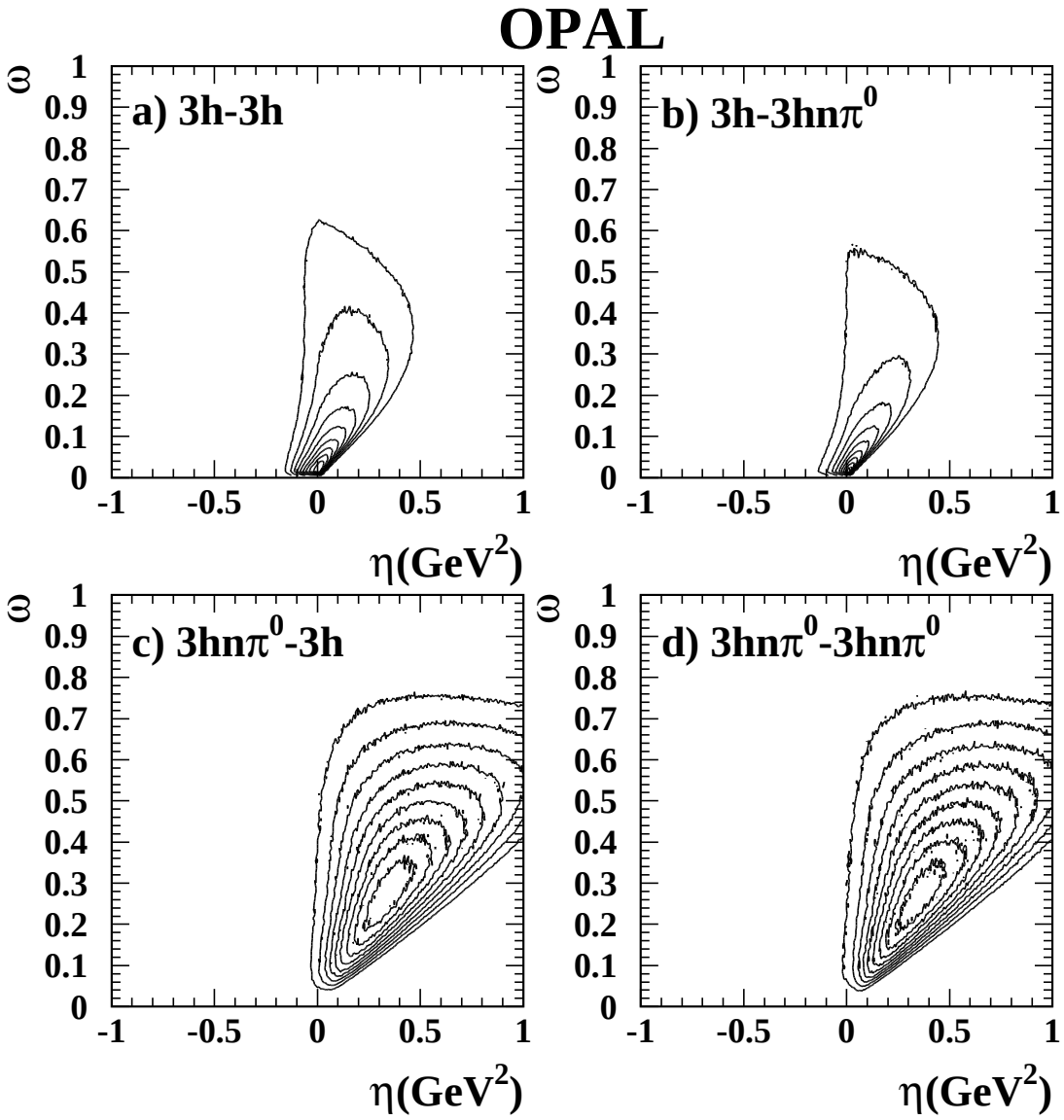

Figure 2: Contour plots of reference histograms of the physics functions. They show ten equidistant levels of probability densities of the physics functions; a) $\mathcal{P}_{3h-3h}$, b) $\mathcal{P}_{3h-3hn\pi^0}$ c) $\mathcal{P}_{3hn\pi^0-3h}$ d) $\mathcal{P}_{3hn\pi^0-3hn\pi^0}$ for $M_{\nu_\tau} = 0$ MeV, where the first channel indicates the decay in the measurement cone and the second represents the decay in the opposite cone.

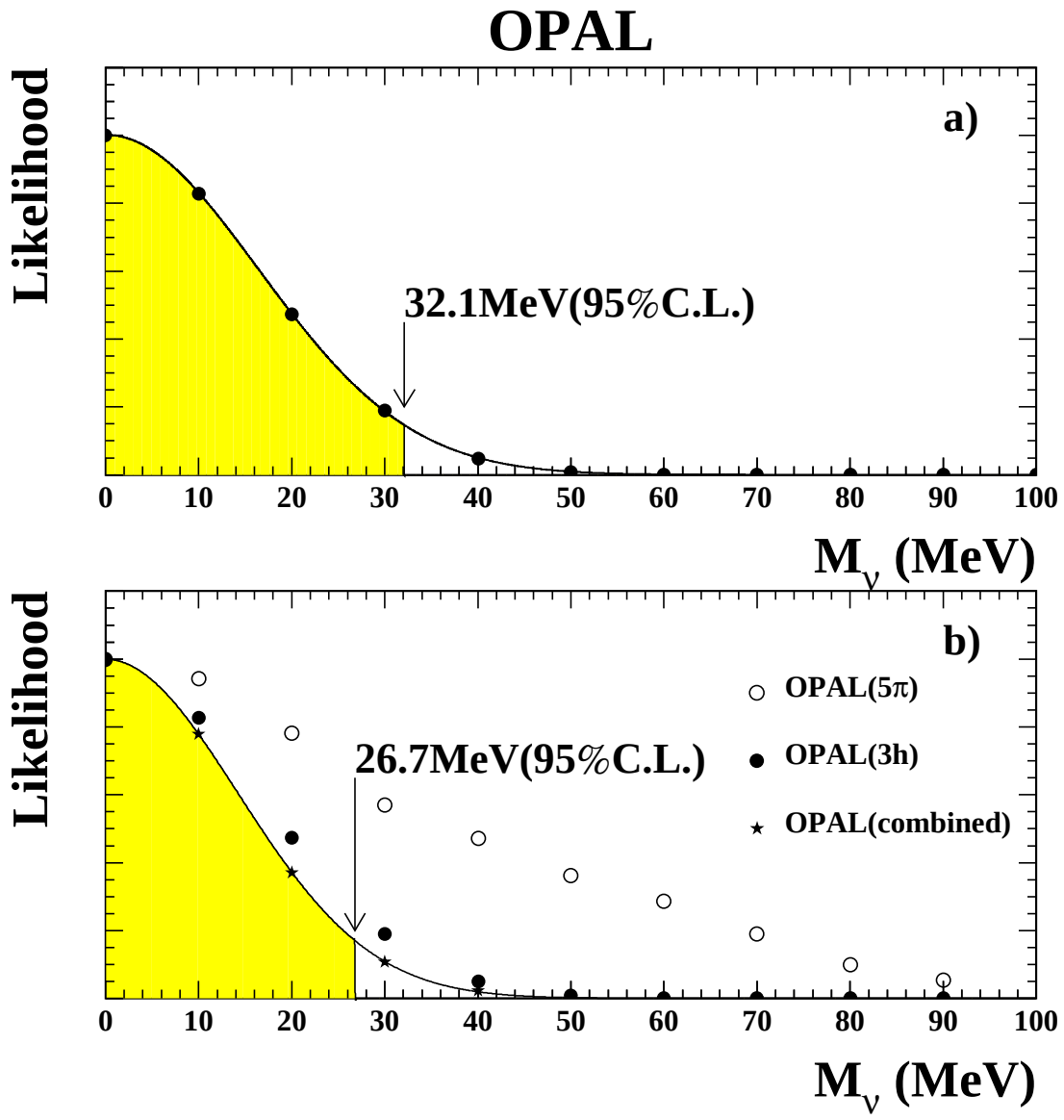

Figure 3: Total likelihood values versus M_{ν_τ} for a) this 2-dimensional analysis using $\tau \to 3h\nu_\tau$ and b) combined with the OPAL $\tau \to 5\pi\nu_\tau$ analysis. Note that the 95% C.L. limits on M_{ν_τ} shown have not been corrected for the effect of systematic uncertainties.